



Chemical looping tar reforming using La/Sr/Fe-containing mixed oxides supported on ZrO₂

Martin Keller^{a,*}, Henrik Leion^a, Tobias Mattisson^b

^a Department of Chemical and Biological Engineering, Chalmers University of Technology, S-412 96 Göteborg, Sweden

^b Department of Energy and Environment, Chalmers University of Technology, S-412 96 Göteborg, Sweden



ARTICLE INFO

Article history:

Received 13 July 2015

Received in revised form 21 October 2015

Accepted 24 October 2015

Available online 28 October 2015

Keywords:

Tar reforming

Chemical-looping reforming

Gasification

Dual fluidized bed

Zirconia

ABSTRACT

Biomass gasification gas contains condensable hydrocarbons usually referred to as “tars”. The use of chemical-looping reforming (CLR) has been proposed as a downstream technology for tar removal from the hot raw gasification gas. In this work two different ZrO₂ support materials impregnated with La, Sr, Fe and mixtures thereof have been investigated as bed material for this proposed CLR process, with benzene and ethylene as tar surrogates. It was found that only combinations of La and Fe yielded significant catalytic activity for benzene conversion that could be further improved by adding Sr. Over this material, the benzene conversion reaction was found to be of first order with respect to benzene, and a simple kinetic model indicates that a high degree of benzene conversion can be obtained at reasonable residence times when the reactor temperature is sufficiently high ($T = 850^\circ\text{C}$). It was also observed that this material exhibited some activity for selective catalytic oxidation of benzene, which could further increase the tar conversion when either the bed material provided oxygen to the gas or a small stream of molecular O₂ was added to the gasification gas feed. XRD analysis of the used bed materials revealed that a pyrochlore phase and SrZrO₃ perovskite were formed during the experiment.

© 2015 Elsevier B.V. All rights reserved.

1. Introduction and background

Gasification of biomass presents a promising route to generate carbon-neutral synthesis gas (CO + H₂), which can then be further processed into valuable gaseous and liquid fuels such as Substitute Natural Gas (SNG), Dimethyl Ether (DME) or others [1–3]. Apart from the desired major syngas compounds, raw gasification gas usually contains impurities and contaminants such as sulphur compounds, ammonia, non-condensable hydrocarbons and condensable hydrocarbons usually referred to as tars [4]. The high condensation temperature of the tar compounds causes them to condense in downstream equipment which may lead to fouling and blocking [5].

It has been proposed to remove these tars by hot catalytic gas cleaning [4,6]. Such a catalytic hot gas tar removal can be realized in various reactor configurations and many different catalytic materials have been tested for their tar removal capability [7]. Most of

these catalytic materials suffer from deactivation due to the formation of coke or sulphides on the catalytically active surface [8,9]. To overcome this problem a process referred to as “chemical looping reforming” (CLR) has been recently proposed, in which the catalyst is continuously regenerated in air [10]. This is achieved by circulating the bed material between a reformer, in which the bed material is contacted with the raw synthesis gas, and a regenerator, in which the bed material is regenerated by oxidizing coke deposits with air. Such a reactor system is illustrated in Fig. 1.

The various reaction pathways, reaction equations and measures to control the oxygen transport and the degree of oxidation of the gasification gas have been discussed in previous publications [10,11].

CLR of tars has been tested in a continuous unit with the natural ore ilmenite [10,12], synthetic Mn₃O₄ supported on ZrO₂ [13] and NiO supported on α -Al₂O₃ [12,14] as bed materials. Although Ni-based oxygen carriers have a high propensity to convert hydrocarbons, nickel is burdened with issues related to toxicity, likely making it highly inappropriate to use in a fluidized bed process. It is thus important to find alternatives to Ni. In a recently published screening study with C₂H₄ as a tar surrogate, supported Cu-based materials and perovskitic La_{0.8}Sr_{0.2}FeO₃ were identified as promising bed materials for CLR [11]. In a more detailed study of these materials, it was recently found that Cu-based materials

Abbreviations: BET, Brunauer–Emmett–Teller; CLR, chemical looping reforming; DME, dimethyl ether; FT-IR, fourier transform infrared; SNG, substitute natural gas; XRD, X-ray diffraction; GHSV, gas hourly space Velocity.

* Corresponding author.

E-mail address: kellerm@chalmers.se (M. Keller).

Nomenclature

γ	Conversion of hydrocarbon
τ	Gas residence time, s
ρ	Density, kg m^{-3}
k	Apparent reaction rate constant, s^{-1}
m	Mass of bed material, kg
\dot{n}	Molar flow rate, mol s^{-1}
T	Reactor temperature, K
T_N	Normal temperature (273.15 K)
\dot{V}	Volumetric gas flow rate in the reactor, $\text{m}^3 \text{s}^{-1}$
x	Molar fraction

Subscripts

in	Gas flowing into the experimental reactor
out	Gas flowing out from the experimental reactor

are unable to convert monoaromatic compounds such as benzene and toluene, while $\text{La}_{0.8}\text{Sr}_{0.2}\text{FeO}_3$ perovskite supported on $\gamma\text{-Al}_2\text{O}_3$ achieved rather high conversion of monoaromatic compounds [15]. These materials are also oxygen carriers, meaning that some oxygen is active for converting tar through non-catalytic partial oxidation.

The previously investigated $\text{La}_{0.8}\text{Sr}_{0.2}\text{FeO}_3/\gamma\text{-Al}_2\text{O}_3$ material has been produced by supporting micrometer-sized $\text{La}_{0.8}\text{Sr}_{0.2}\text{FeO}_3$ pre-produced powder on the outside of larger $\gamma\text{-Al}_2\text{O}_3$ particles, leading to a rather small active $\text{La}_{0.8}\text{Sr}_{0.2}\text{FeO}_3$ surface area.

The aim of the work presented here is to investigate the performance of $\text{La}_{0.8}\text{Sr}_{0.2}\text{FeO}_3$ supported on ZrO_2 produced by incipient wetness impregnation. Impregnation can potentially provide a larger active surface area due an increased dispersion of the active phase on a substrate. ZrO_2 was chosen as a support material due to its relative chemical inertness, demonstrated by its use as a support for perovskites as a cathode material for solid oxide fuel cells [16], and its reported activity for selective catalytic oxidation of tars [17]. For this study, two different ZrO_2 supports were impregnated with individual metals La, Fe and Sr and combinations thereof corresponding to LaFeO_3 and $\text{La}_{0.8}\text{Sr}_{0.2}\text{FeO}_3$ perovskites. Benzene and ethylene were used as tar surrogates. In previous work on CLR it was found that benzene is commonly the hardest aromatic compound to convert. In fact, benzene is often formed as a product of the cracking of larger polyaromatic compounds [12]. Ethylene is used as a tar surrogate because it is an indicator for the ability of bed materials to convert tars likely due to the π bonds of ethylene being similar to those found in aromatic tars [18]. Not only is the conversion of these two compounds of interest as tar surrogates, but

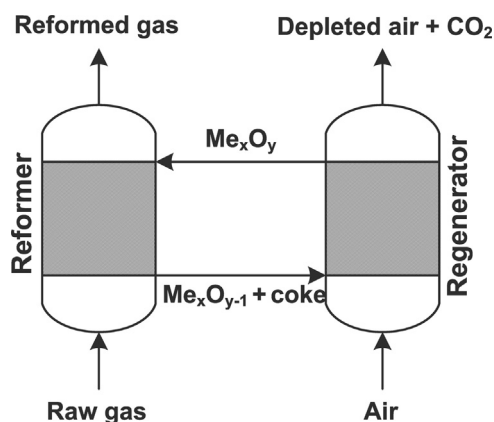


Fig. 1. Schematic of the chemical looping reforming process for tar removal from biomass producer gas.

Table 1

Composition of synthetic gasification gas mixtures used in the experiments.

Concentration in % mol	Chemical looping reforming experiments	Selective catalytic oxidation experiments (SCO)
H_2O	25	25
CO	10.75	10.75
CO_2	3.73	3.73
H_2	5.78	5.78
CH_4	3.5	3.5
C_2H_4	1.25	1.25
C_6H_6	0–1.4	1.4
O_2	–	1–2.5
N_2	Balance	Balance

both of them are also found in significant quantities in raw gasification gas from dual fluidized bed biomass gasification, and represent removal challenges [19]. Simple reaction kinetics for the catalytic conversion of benzene were determined for both materials, and the suitability of the material for selective catalytic oxidation was investigated.

2. Experimental

2.1. Experimental setup and procedure

Experiments were conducted in a small-scale fluidized bed reactor and the experimental setup is illustrated in Fig. 2. A detailed description of this experimental setup can be found in a previous publication [11]. Experiments were conducted with 9 g of bed material sieved to a size range of 125–250 μm . Additionally, empty reactor experiments were conducted to determine the extent of homogeneous gas phase reactions which could not be attributed to the bed material. To emulate the circulation of the bed material between the regenerator and the reformer of a continuous CLR unit as described in Fig. 1, the bed material was alternately exposed to reducing and oxidizing conditions in a cyclic manner. In between these exposures, the reactor was flushed with N_2 for 180 s. Reducing conditions in the reformer were emulated by a synthetic gasification gas flow of 1 $\text{L}_\text{N}/\text{min}$ for 1000 s. The composition of these gas mixtures is shown in Table 1. For some experiments the concentration of benzene was varied between 0 and 1.4 mol% and for the selective catalytic oxidation (SCO) experiments 1% and 2.5 mol% O_2 were added to the gas. After the exposure of the bed material to the reducing gas, the reactor was flushed with N_2 and then the bed material was exposed to a flow of 0.6 $\text{L}_\text{N}/\text{min}$ of synthetic air (consisting of 20.9% O_2 in N_2) for 360 s in order to emulate the oxidizing conditions in the regenerator and to achieve full reoxidation and regeneration of the bed material. The system was operated at atmospheric pressure and the temperature was varied between 750 °C and 850 °C. Experimental cycles were repeated three times to ensure reproducibility. Unless indicated otherwise, the data presented here are averages of the three cycles.

2.2. Gas analysis

The wet effluent gas was transported in heated lines to a Thermo-Scientific iS50 FT-IR analyzer equipped with a heated gas cell. The FT-IR analyzer was carefully calibrated for the quantification of the concentration of CO , CO_2 , H_2O , CH_4 , C_2H_4 , C_2H_6 , and C_6H_6 by conducting calibration experiments with both pure gases diluted in N_2 and various wet and dry gas mixtures. In total, over 200 calibration compositions were generated and evaluated in order to obtain accurate measurements. Gas concentrations were measured every 4 s with the FT-IR. After the gas was cooled and the condensate removed from the gas stream, the dry effluent gas

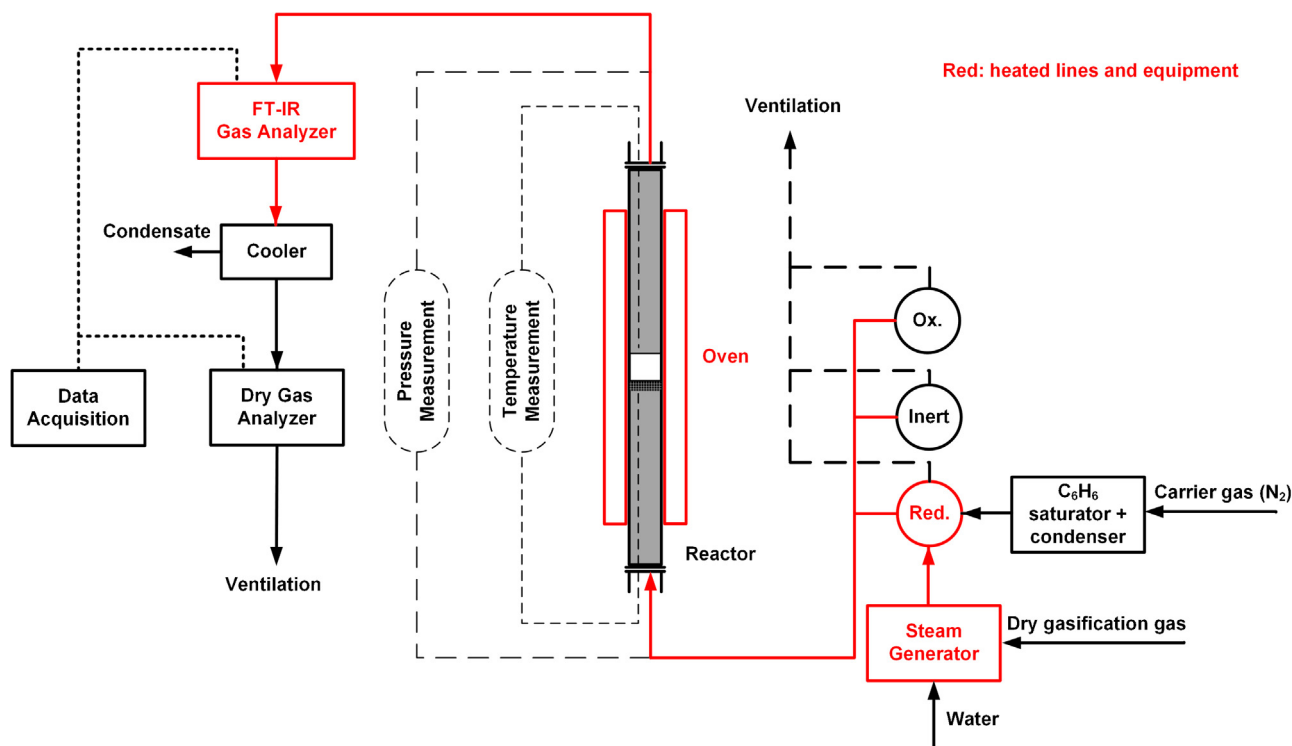


Fig. 2. Schematic overview of the experimental setup.

Table 2
Overview over bed materials used in this study.

Code	Composition
ZNANO	Unimpregnated monoclinic ZrO ₂ manufactured from ZrO ₂ nanoparticles
ZTECH	Unimpregnated plasma-processed monoclinic ZrO ₂
ZNANO.LaSrFe	Metal loading corresponds to 10 wt% La _{0.8} Sr _{0.2} FeO ₃ on support
ZTECH.LaSrFe	Metal loading corresponds to 10 wt% La _{0.8} Sr _{0.2} FeO ₃ on support
ZTECH.LaFe	Metal loading corresponds to 10 wt% LaFeO ₃ on support
ZTECH.La	Same molar amount of La as for ZTECH.LaSrFe
ZTECH.Sr	Same molar amount of Sr as for ZTECH.LaSrFe
ZTECH.Fe	Same molar amount of Fe as for ZTECH.LaSrFe

was then sent to a dry gas analyzer to determine the concentration of H₂ and O₂ with a thermal conductivity and a paramagnetic gas sensor.

2.3. Bed materials

Bed materials were prepared by incipient wetness impregnation of aqueous metal nitrate solutions on ZrO₂ support materials. Aqueous metal nitrate solution was prepared with its volume corresponding to two times the pore volume of the particles. This solution was then added to the particles dropwise under continuous stirring at room temperature in two steps with intermediate drying. Two different support materials were investigated in order to determine the influence of the support microstructure on benzene and ethylene conversion. One support material was a commercial, plasma processed monoclinic zirconia (Z-TECH LLC). This material provides porosity for impregnation since it exhibits a dendritic structure composed of zirconia crystals that are about 0.2 μm in size. This support material is abbreviated as ZTECH

throughout this article. The second support material was produced from zirconia nanopowder (Inframat Advanced Materials LLC, avg. particle size 38 nm, BET surface area 26.5 m²/g) by slurring it with organic binder and alcohol, drying, calcination at 700 °C for 4 h and subsequent crushing and sieving to the desired size range. This support material is abbreviated as ZNANO throughout this article. The ZNANO support was then impregnated with a metal nitrate aqueous solution containing metal nitrates that correspond to 10 wt% La_{0.8}Sr_{0.2}FeO₃ supported on ZNANO in the final product. To investigate the influence of the individual metals on the reactivity of ZrO₂ based materials, the ZTECH support material was not only impregnated with metal nitrates that correspond to 10 wt% La_{0.8}Sr_{0.2}FeO₃, but also with nitrates corresponding to 10 wt% LaFeO₃, and with individual La, Sr and Fe metal nitrates corresponding to the same molar amount of the corresponding metal that is included in the 10 wt% La_{0.8}Sr_{0.2}FeO₃ materials. A list of the prepared materials and the code by which they are referred to in this article is provided in Table 2. All impregnated materials and also the non-impregnated support materials that have been investigated as reference materials were then calcined at 850 °C for 20 h in a muffle furnace in air. The purpose of this heat treatment is to decompose the metal nitrates and form the desired metal oxides.

2.4. Characterization of bed materials

The BET surface area and pore volume distribution of the bed materials were determined by N₂ adsorption (Micromeritics, TriStar 3000) before and after the experiments. The major crystalline phases of the bed materials were identified before and after the experiments using powder X-ray diffraction (Bruker D8 advance) with CuKα radiation. Bed materials were furthermore characterized by Scanning Electron Microscopy with Energy Dispersive Spectroscopy (SEM/EDS).

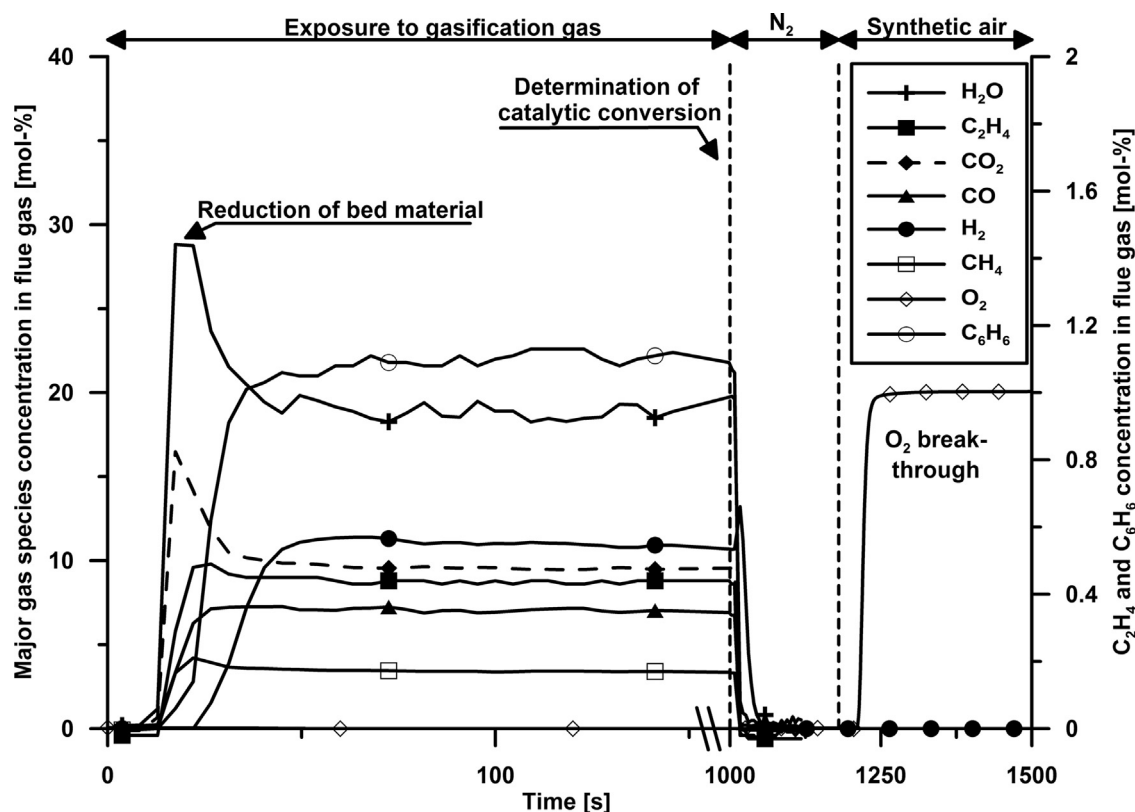


Fig. 3. Recorded gas concentration profile during exposure to gasification gas with 1.4 % C₆H₆ in feed and subsequent reoxidation in air of ZTECH.LaSrFe at a temperature of $T=800\text{ }^{\circ}\text{C}$ (Note that the x-axis is broken after the gas concentrations stabilize after 150 s).

2.5. Data evaluation

The conversion of the various hydrocarbons C_xH_y , $\gamma_{C_xH_y}$, is calculated from a molar balance of the inlet C_xH_y and the outflowing C_xH_y as determined by FT-IR measurement.

$$\gamma_{C_xH_y} = \frac{x_{C_xH_y, \text{in}} \dot{n}_{\text{in}} - x_{C_xH_y, \text{out}} \dot{n}_{\text{out}}}{x_{C_xH_y, \text{in}} \dot{n}_{\text{in}}} \times 100\% \quad (1)$$

The degree of gas oxidation ϕ , which describes to which degree the synthetic gasification gas is oxidized by oxygen supplied by the bed material or as molecular oxygen, is calculated from the oxygen required for full oxidation of the gas.

$$\phi = 1 - \frac{\left(\frac{1}{2} x_{\text{CO}, \text{out}} + \frac{1}{2} x_{\text{H}_2, \text{out}} + 2 x_{\text{CH}_4, \text{out}} + 3 x_{\text{C}_2\text{H}_4, \text{out}} + 7.5 x_{\text{C}_6\text{H}_6, \text{out}} \right) \times \dot{n}_{\text{out}}}{\left(\frac{1}{2} x_{\text{CO}, \text{in}} + \frac{1}{2} x_{\text{H}_2, \text{in}} + 2 x_{\text{CH}_4, \text{in}} + 3 x_{\text{C}_2\text{H}_4, \text{in}} + 7.5 x_{\text{C}_6\text{H}_6, \text{in}} \right) \times \dot{n}_{\text{in}}} \quad (2)$$

3. Results

3.1. Gas concentration profiles

In Fig. 3 the recorded gas concentration profiles are shown with ZTECH.LaSrFe as a bed material and 1.4 % C₆H₆ in the gasification gas at $T=800\text{ }^{\circ}\text{C}$. In the beginning, the fully oxidized bed material is exposed to gasification gas and thus reduced. It oxidizes the gasification gas, resulting in a peak in H₂O and CO₂ concentrations. Once these concentrations stabilize the material has reached its thermodynamically stable state and the bed material does not provide oxygen to the gas any longer. Afterwards the reactor is first flushed with N₂ and then synthetic air is introduced to the reactor, resulting in an oxidation of possible coke deposits and a reoxidation of the bed material. In all experiments the amount of coke formed on the bed material after 1000 s of exposure to the gasification gas was small and the resulting CO₂ peak from its combustion was

detectable, but is not visible in this plot. During all experiments, no other hydrocarbons than the ones shown in Fig. 3 were detected. The catalytic conversion of the different hydrocarbons species is determined during the stable period from 500 to 1000 s in which no oxygen is transferred from the particles to the gas phase any longer. There is a transient period of partial oxidation between the region of full oxidation of the fuel and the region of only catalytic effects, which is also analyzed in this work.

3.2. Catalytic conversion of C₆H₆ over La, Sr, Fe-impregnated ZTECH support

In Fig. 4a the conversion of C₆H₆ and in Fig. 4b the conversion of C₂H₄ are shown as a function of reactor temperature for the different ZTECH impregnated materials and for an empty reactor experiment. It should be noted that the data points presented in Figs. 4, 8, 9 and 11 are averages of 3 oxidation/reduction cycles, and in none of the experiments was a change of reactivity of the bed material with cycle observed. It is evident from Fig. 4a that the ZrO₂ support itself does not convert benzene. The impregnation with only Fe or Sr (ZTECH.Sr, ZTECH.Fe) yields no significant benzene conversion either. ZTECH.La exhibited some marginal improvement of benzene conversion at $T=850\text{ }^{\circ}\text{C}$. However, only ZTECH.LaFe and ZTECH.LaSrFe exhibit significant and rather high degrees of benzene conversion. When comparing ZTECH.LaFe and ZTECH.LaSrFe it can be seen that the addition of Sr greatly improves the benzene conversion. Similar trends that were observed for the benzene conversion could be observed for the ethylene conversion, with the exception that ZTECH.Fe exhibits a significantly higher conversion than the unimpregnated support and ZTECH.Sr.

In Fig. 5 the three XRD patterns of ZTECH.LaSrFe (1) before the experiment after calcination, (2) after the experiment and quenched in N₂ gas after the exposure to gasifications gas at $800\text{ }^{\circ}\text{C}$,

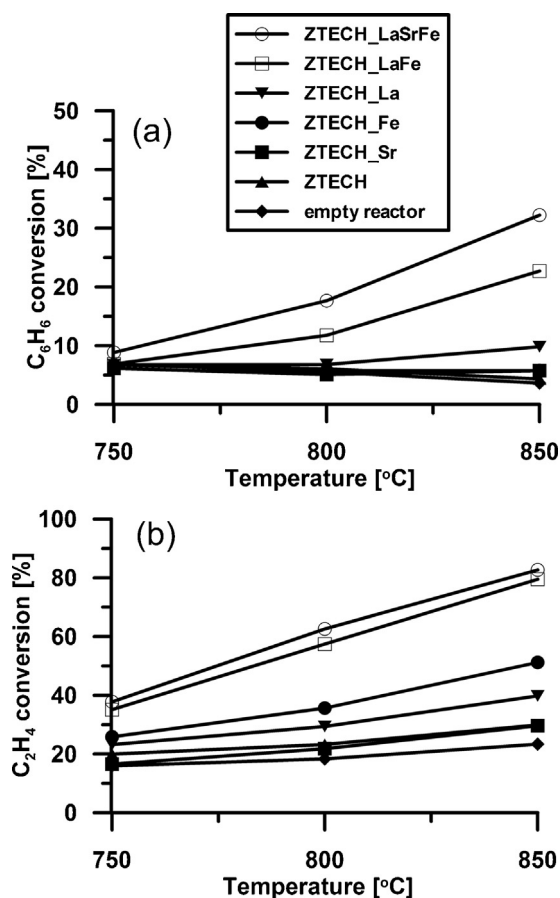


Fig. 4. Conversion of (a) C_6H_6 and (b) C_2H_4 as a function of reactor temperature with 1.4% C_6H_6 in the gas feed for the different ZTECH impregnated materials and for an empty reactor experiment.

and (3) after that material had been reoxidized in air at 800 °C for 1 h. After calcination, only monoclinic ZrO_2 , a $ZrSiO_4$ impurity and perovskitic $La_{0.8}Sr_{0.2}FeO_3$ phases could be observed. During the experiment the $La_{0.8}Sr_{0.2}FeO_3$ perovskite phase decomposed and reacted with the ZrO_2 support to form $La_2Zr_2O_7$ pyrochlore and minor quantities of $SrZrO_3$ perovskite. Even after reoxidation at 800 °C in air, the $La_{0.8}Sr_{0.2}FeO_3$ perovskite phase could not be

Table 3

Phases other than monoclinic ZrO_2 and $ZrSiO_4$ impurity identified by XRD before the bed material was used and after the experiment had been stopped after exposure to gasification gas at $T = 800$ °C.

Material	Phases identified by XRD before experiment	Phases identified by XRD after experiment, reduced
ZTECH.LaSrFe	$La_{0.8}Sr_{0.2}FeO_3$	$La_2Zr_2O_7$, $SrZrO_3$
ZTECH.LaFe	$LaFeO_3$	$La_2Zr_2O_7$, $LaFeO_3$ (minor)
ZTECH.La	None	None
ZTECH.Sr	$SrZrO_3$	$SrZrO_3$
ZTECH.Fe	Fe_2O_3	None

restored, as is evident from the XRD pattern after reoxidation. The identified phases for the other ZTECH impregnated materials before and after the experiment are summarized in Table 3. It is interesting to observe that the impregnation with La and Fe only, ZTECH.LaFe, resulted in a more stable perovskite phase $LaFeO_3$, which did not entirely decompose when exposed to the reducing experimental conditions. However, also on ZTECH.LaFe did major amounts of pyrochlore $La_2Zr_2O_7$ form, leaving only a small quantity of $LaFeO_3$ intact. Furthermore, it was observed that on ZTECH.La, no crystalline pyrochlore phase was formed either during calcination or during the experiment. This indicates that the presence of Fe facilitates the formation of a pyrochlore phase.

3.3. Comparison of ZTECH.LaSrFe and ZNANO.LaSrFe as support materials

In order to determine the influence of support material on the reactivity of ZrO_2 -supported LaSrFe impregnated materials, two different ZrO_2 support materials were investigated with largely different properties. Results of the surface area and pore volume distribution determination by N_2 adsorption of the two fresh unimpregnated support materials, the La/Sr/Fe impregnated and calcined materials and the materials retrieved from the reactor after the experiments are summarized in Table 4. In Fig. 6, the cumulative pore volume as a function of pore width for these materials is shown. It could be observed that the BET surface area and the pore volume of the fresh ZNANO is significantly larger than that of the fresh ZTECH support. From Fig. 6, it can be seen that most of the pore volume of fresh ZNANO is found in pores of about 30–100 nm in size. This is to be expected considering that the average particle size of the primary ZrO_2 nanopowder used in the synthesis is about 38 nm. Some of this initially higher mesoporosity and surface area

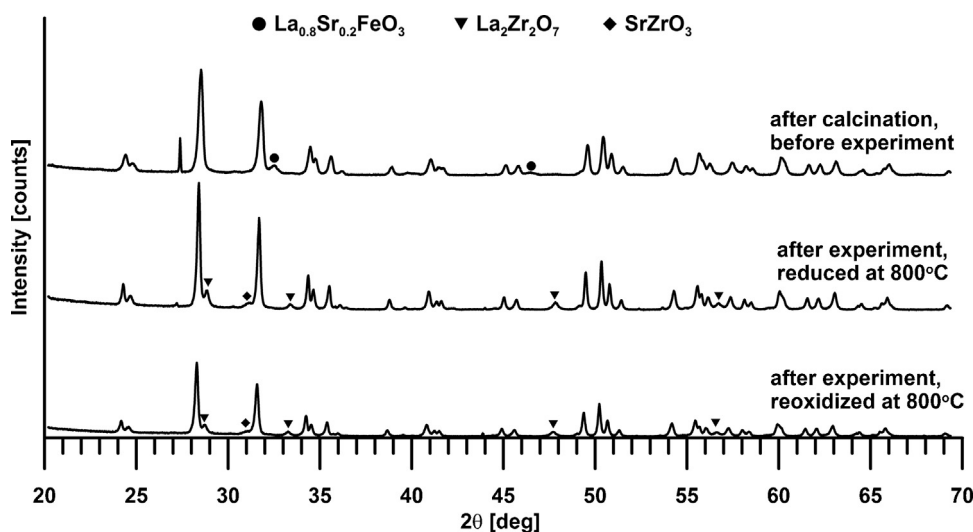


Fig. 5. XRD patterns of ZTECH.LaSrFe before the experiment, after the experiment and reduced at 800 °C and after reoxidation in air at 800 °C for 1 h.

Table 4

Results of BET analysis of the two fresh support materials ZTECH and ZNANO, ZTECH.LaSrFe and ZNANO.LaSrFe after impregnation and calcination and used ZTECH.LaSrFe and ZNANO.LaSrFe obtained from the reactor after the experiments.

Material	BET surface area [m ² /g]	Pore volume [ml/g]	Average pore width [nm]
ZTECH fresh	6.90	0.031	15.36
ZTECH.LaSrFe, impregnated and calcined	5.45	0.030	21.77
ZTECH.LaSrFe after experiment	4.48	0.020	15.11
ZNANO fresh	27.83	0.164	19.28
ZNANO.LaSrFe, impregnated and calcined	19.19	0.117	22.98
ZNANO.LaSrFe after experiment	6.50	0.025	12.33

of the fresh ZNANO support pore volume and surface area is lost during the calcination for 20 h at 850 °C. During the experiment the surface area and mesoporosity of the ZNANO based material decreases further, and after the experiment the used ZNANO.LaSrFe and ZTECH.LaSrFe exhibit very similar BET surface areas and pore volume distributions.

The tapped bulk density of used ZNANO.LaSrFe was determined to be 1.02 g/ml, whereas the tapped bulk density of used ZTECH.LaSrFe was 2.48 g/ml and thus significantly higher. In Fig. 7a and b, SEM images of a used ZTECH.LaSrFe particle are shown. The close-up in Fig. 7b shows that the porous structure of the ZTECH support is maintained throughout the experiments, with pore sizes around 0.1–0.3 μm observable. In Fig. 7c and d a used ZNANO.LaSrFe particle is shown, and it can be observed that the pore structure consists mostly of larger micron-sized micropores. This difference in pore size together with the irregular shape of the ZNANO particles may explain the difference in bulk density observed for the ZTECH and ZNANO materials.

In Fig. 8 the benzene conversion and the ethylene conversion over these two materials is compared. Since the same mass of bed material was used in both experiments, the comparison is mass-based. It can be seen that in a mass-based comparison ZNANO.LaSrFe achieved a higher degree of both benzene and ethylene conversion.

3.4. Determination of apparent reaction kinetics for benzene reforming

Experiments with variable C₆H₆ concentration in the feed were conducted with ZNANO.LaSrFe in order to determine apparent reaction kinetics and the reaction order of the benzene reforming reaction with respect to benzene concentration. The benzene inlet concentration was varied between 0.1 and 1.4 %. It was found that the conversion of benzene is constant around 25% and not a function of C₆H₆ inlet concentration, indicating that the kinetics of the benzene reforming reaction are of first order with respect to benzene concentration. Due to the first-order nature of this reaction, apparent reaction rate constants can be easily obtained when assuming plug flow and neglecting the rather small volume expansion of the gas in the reactor.

$$k = - \frac{\ln \left(1 - \frac{\gamma_{C_6H_6}}{100} \right)}{\tau} \quad (3)$$

Here, $\gamma_{C_6H_6}$ denotes the conversion of benzene and τ denotes the gas residence time that has been approximated by using the bulk density of the bed material, the mass of the bed material and the volumetric flow rate in the reactor.

$$\tau = \frac{m_{\text{bedmaterial}}}{e_{\text{bulk, bedmaterial}} \dot{V}} \quad (4)$$

In Fig. 9 the Arrhenius plot of the apparent reaction rate constant over inverse temperature for ZTECH.LaSrFe and ZNANO.LaSrFe is shown. It can be observed that this bed volume-based comparison

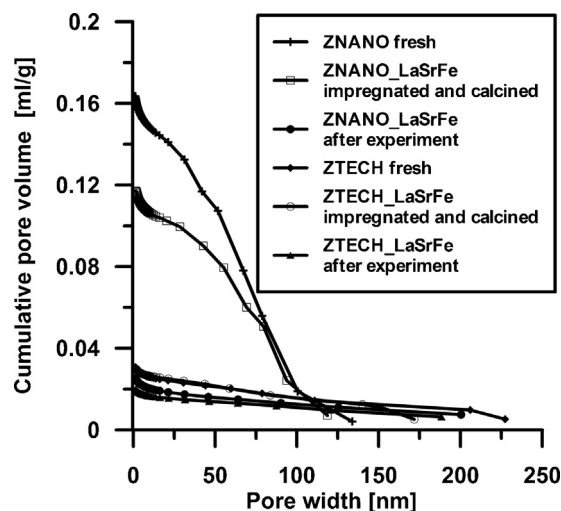


Fig. 6. Cumulative pore volume over pore width obtained by N₂ adsorption for fresh ZTECH and ZNANO, ZTECH.LaSrFe and ZNANO.LaSrFe after impregnation and calcination and used ZTECH.LaSrFe and ZNANO.LaSrFe obtained from the reactor after the experiments.

yields a slightly higher reaction rate over ZTECH.LaSrFe than over ZNANO.LaSrFe. The activation energies for both materials were found to be rather similar, with 142.8 kJ/mol for ZTECH.LaSrFe and 185.5 kJ/mol for ZNANO.LaSrFe.

3.5. Activity of catalyst for selective catalytic oxidation (SCO) of benzene

In the experiments conducted for this work, the oxidized bed material provides some oxygen to the gasification gas in the very beginning of the exposure to the gasification gas to fully oxidize the gas, as illustrated in Fig. 3. Then, a short period of partial oxidation of the gasification gas follows. To prolong the periods of full and partial oxidation of the gas and to be able to discern actual partial oxidation from transient effects in the measurement system, experiments were conducted with only 25% wet gasification gas and 75% N₂ in the feed. The results of these experiments are exemplary shown for $T = 800$ °C in Fig. 10, where the conversion of hydrocarbons over ZNANO.LaSrFe as a function of the degree of gasification gas oxidation is displayed. Here $\phi = 1$ corresponds to complete combustion, while at $\phi = 0$ there would be no oxygen transferred to the gas. It can be observed that the C₂H₄ conversion and the CH₄ conversion does not increase during the partial oxidation of the gas by the bed material. In fact, a small amount of CH₄ seems to be generated during partial oxidation. Only at very high values of ϕ an increase CH₄ conversion is observed. On the other hand, the conversion of benzene is significantly increased already at small values of ϕ when

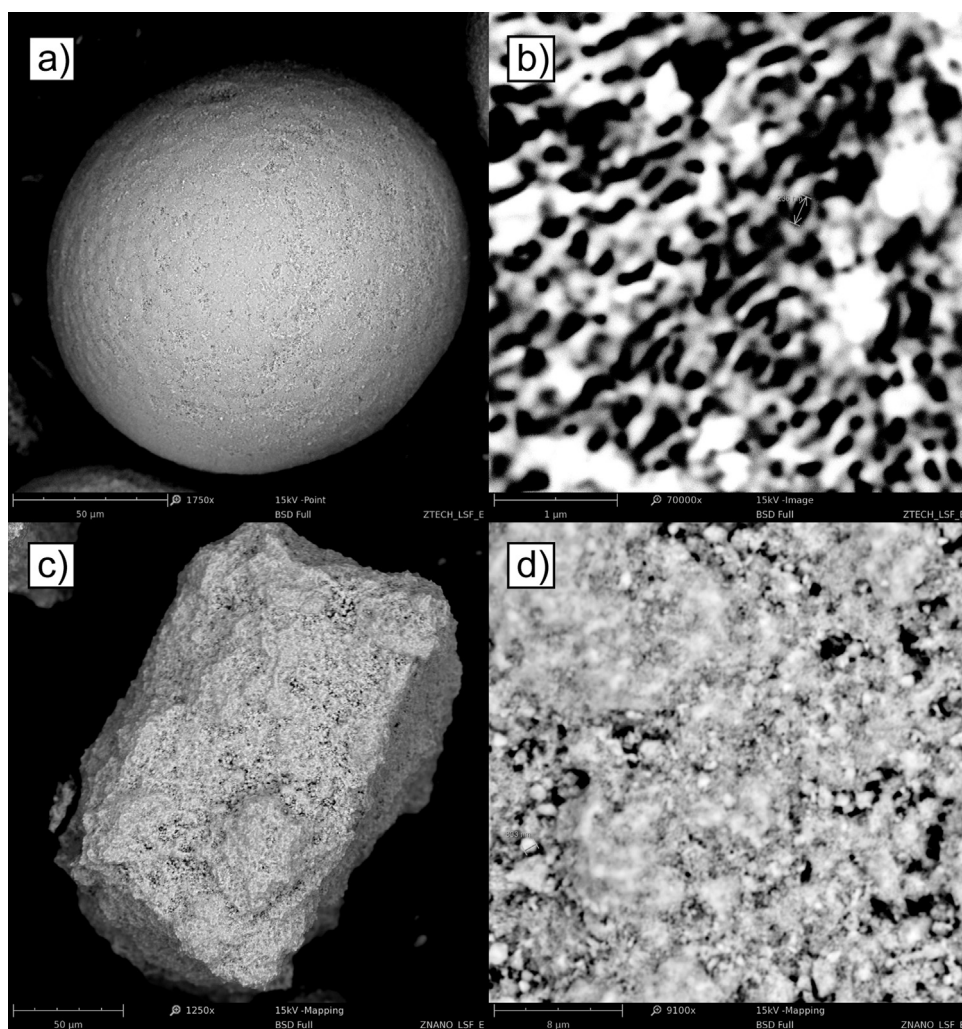


Fig. 7. SEM images of a used ZTECH.LaSrFe particle retrieved from the reactor (a + b) and of a used ZNANO.LaSrFe particle (c + d).

only a limited amount of oxygen is provided by the bed material.

To confirm this finding and to determine if there is an influence of the mode of oxygen provision to the gas (via the bed material or via gas phase molecular oxygen) on hydrocarbon conversion, experiments with O_2 co-feeding were conducted for this work.

In Fig. 11 the conversion of C_6H_6 and C_2H_4 over ZNANO.LaSrFe as a function of reactor temperature with 1.4 % C_6H_6 in the gas feed and 0, 1, or 2.5% O_2 in the gasification gas feed is shown. From Fig. 11a it can be observed that the benzene conversion increases with the amount of O_2 fed at all temperatures. This effect, relative to the catalytic conversion in the absence of O_2 , is most pronounced at $T=750^\circ C$, at which the addition of 2.5% O_2 increases the benzene conversion from about 7% to 28%. The ethylene conversion increases somewhat when O_2 is introduced to the feed at $T=750^\circ C$, but remains unchanged at $T \geq 800^\circ C$.

Since all of the oxygen reacts, the co-feeding of 1% and 2.5% O_2 with the gasification gas corresponds to $\phi=0.034$ and $\phi=0.085$, respectively. The finding of a slight increase of benzene conversion thus confirms the previously observed trend during partial oxidation of the gas by the bed material as shown in Fig. 10. It also indicates that the different modes of oxygen provision, via the bed material or via the co-feeding of molecular oxygen, result in a somewhat comparable increase of benzene conversion.

4. Discussion

The results presented in Fig. 4 together with the results of the XRD analysis of the materials indicate that only the impregnation with La and Fe yields materials with a significant catalytic activity for benzene reforming; however this catalytic activity does not seem to require the existence of a crystalline $La_{1-x}Sr_xFeO_3$ phase, since the ZTECH.LaSrFe material exhibits high catalytic activity without such a phase being present during the experiment. The high catalytic activity could originate from the formation of a doped $La_2Zr_2O_7$ phase or an interaction of the $La_2Zr_2O_7$ with amorphous Fe oxide.

When comparing two different ZrO_2 support materials ZNANO and ZTECH impregnated with La, Sr and Fe, it was found that, in a mass-based comparison, ZNANO.LaSrFe achieved a higher degree of both benzene and ethylene conversion. It is conceivable that this is due to a longer gas residence time in the fluidized bed as a result of a higher macroporosity and thus a lower bulk density of ZNANO.LaSrFe particles.

The first order reaction kinetics for the catalytic benzene conversion obtained in this work allow for the prediction of benzene conversion as a function of the gas hourly space velocity based on static bed volume, GHSV, defined as:

$$GHSV = \frac{T_N}{T} \frac{1}{\tau} \quad (5)$$

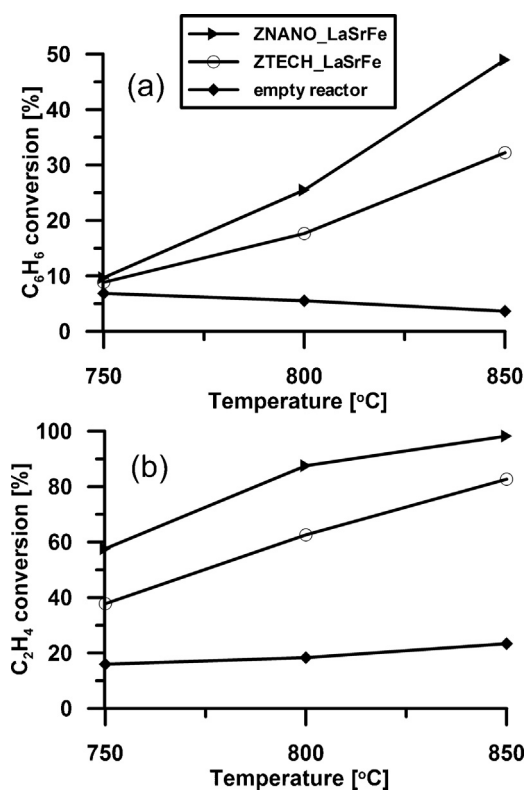


Fig. 8. Conversion of (a) C_6H_6 and (b) C_2H_4 as a function of reactor temperature with 1.4 % C_6H_6 in the gas feed for ZTECH.LaSrFe, ZNANO.LaSrFe and for an empty reactor experiment.

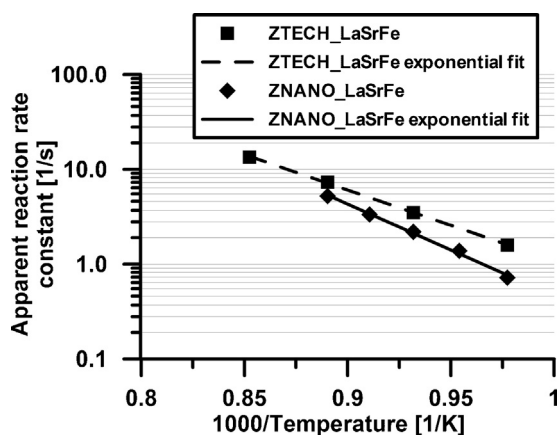


Fig. 9. Arrhenius plot of the apparent reaction rate constant over inverse temperature for ZTECH.LaSrFe and ZNANO.LaSrFe.

Such a prediction is shown for ZTECH.LaSrFe in Fig. 12. It can be observed that, in order to achieve a high degree of benzene conversion at reasonable residence time, a rather high reactor temperature is required.

Kaisalo et al. recently measured aromatic tar conversion over nickel-based and precious metal-based catalysts under similar conditions at about $T=850^\circ C$, however in the presence of potential catalyst poisons H_2S and NH_3 and in a fixed bed reactor [20]. With the nickel catalyst, over 90% tar conversion at a GHSV of $5400\ h^{-1}$ was observed, and with the precious metal catalyst over 60% tar conversion at a GHSV of $12,300\ h^{-1}$ was observed. In comparison, as can be seen from Fig. 12, at $T=850^\circ C$ over ZTECH.LaSrFe a benzene conversion of about 70% is predicted at a GHSV of $5400\ h^{-1}$

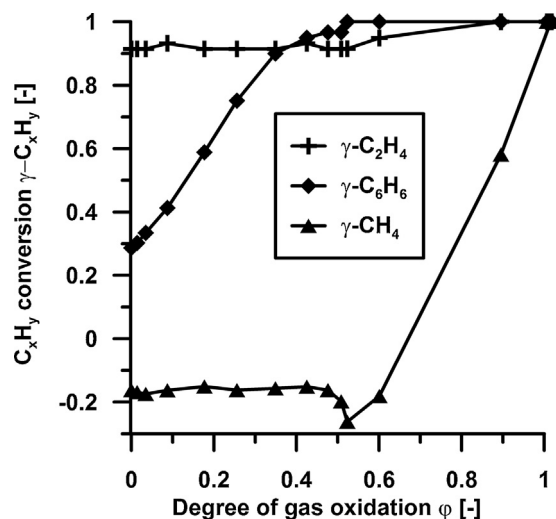


Fig. 10. Hydrocarbon conversion as a function of degree of gas oxidation at $T=800^\circ C$ over ZNANO.LaSrFe with 25% wet gasification gas mixture and 75% N_2 in the feed. The negative conversion values for methane indicate formation of CH_4 .

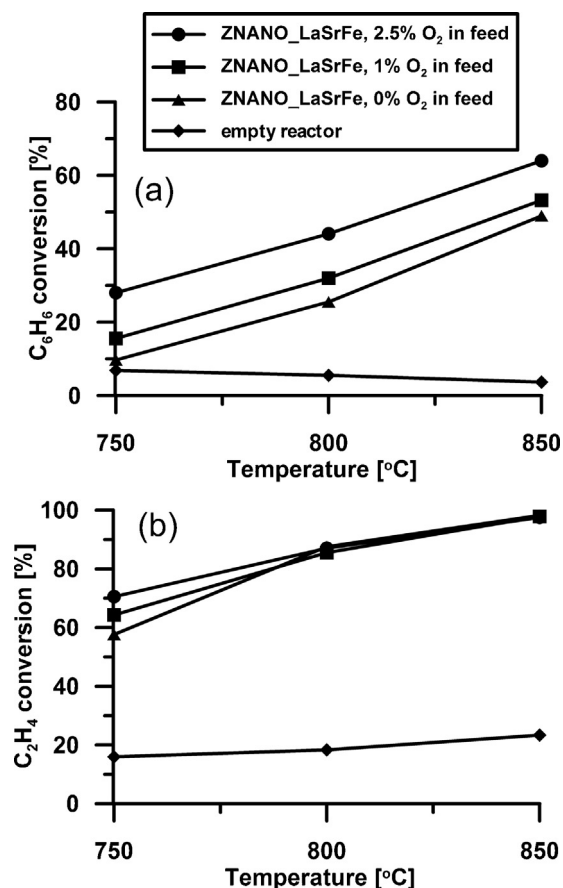


Fig. 11. Conversion of (a) C_6H_6 and (b) C_2H_4 over ZNANO.LaSrFe as a function of reactor temperature with 1.4 % C_6H_6 in the gas feed and 0, 1, or 2.5% O_2 in the gasification gas feed.

and about 40% at a GHSV of $12,300\ h^{-1}$. The expected degree of conversion is thus somewhat lower than over Ni-based materials and precious metal based materials. Furthermore, it is yet unclear whether sulfur and ammonia would have a detrimental effect on the catalytic activity of the materials if they were to be used in a

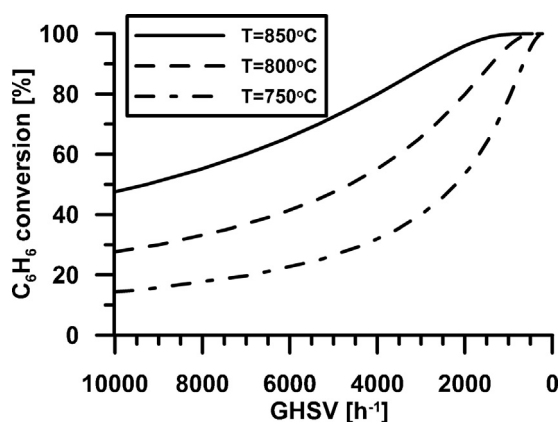


Fig. 12. Prediction of benzene conversion over ZTECH.LaSrFe as a function of gas hourly space velocity GHSV for three different temperatures, using simple kinetic model.

process with continuous catalyst regeneration such as CLR. Nevertheless, considering the expected lower costs compared to precious metal catalysts and the toxicity issue of nickel-based catalysts, the catalysts investigated in this work appear very promising.

The catalytic benzene conversion could be further increased by selective oxidation, either by the co-feeding of molecular oxygen or by oxygen transport by the circulating bed material. ZrO₂ and ZrO₂-based catalysts have been previously investigated for their ability to selectively oxidize tar compounds such as toluene and naphthalene [17,21]. It was found that ZrO₂ is able to selectively oxidize both toluene and naphthalene to some extent when up to 3 % O₂ is added to the gasification gas. In chemical looping tar reforming, oxygen is preferentially provided via oxygen transport by the bed material, and not by the addition of molecular oxygen, as illustrated in Fig. 1. The advantage of such an oxygen transport is that neither N₂ from air dilutes the product gas, nor is a separate Air Separation Unit (ASU) necessary to generate pure oxygen. In this work, it was demonstrated that both the co-feeding of molecular oxygen and the partial oxidation by oxygen provided by the circulating bed material can enhance the benzene conversion to some extent. However, the results shown in Figs. 10 and 11 also indicate that a rather large amount of oxygen needs to be provided to achieve a substantial increase in benzene conversion.

In any case, the provision of O₂ to the gasification gas does result in a significant decrease in the heating value of the product gas, independently of how the oxygen is provided to the gasification gas. In this light, it appears more desirable to aim at increasing the catalytic conversion of benzene without providing too much oxygen to the gas in order to retain the heating value of the gasification gas. This could be achieved, e.g., by increasing gas residence time, as shown in Fig. 12, or by further optimizing the catalytic activity of the bed material.

5. Conclusions

In this study ZrO₂-supported bed materials were investigated with respect to their tar removal capabilities in a chemical looping reforming system with benzene and ethylene as tar surrogates. ZrO₂ was impregnated with individual metals La, Fe and Sr and combinations thereof corresponding to LaFeO₃ and La_{0.8}Sr_{0.2}FeO₃ perovskites, and it was found that only combinations of La and Fe yield significant conversion of benzene. The addition of Sr to La and Fe proved to be very beneficial for benzene conversion, despite the fact that the perovskite La_{0.8}Sr_{0.2}FeO₃ was found to be not stable under reducing conditions and La₂Zr₂O₇ pyrochlore and minor quantities of SrZrO₃ perovskite were formed by interaction with

the ZrO₂ support. For the two different support materials ZNANO and ZTECH impregnated with La, Sr, and Fe simple reaction kinetics were obtained, and it was found that the benzene removal reaction is of first order in regard to benzene concentration. Predictions using this model showed that high benzene conversion can be obtained at reasonable residence times when the reactor temperature is sufficiently high. The benzene conversion can be further improved by transferring oxygen to the gas, either directly from the oxygen carrier particles or by addition of gaseous O₂ to the reactor. However, this leads to oxidation of the gas, thus lowering the heating value of the final product. Hence it appears more desirable to increase the gas residence time in order to increase benzene conversion.

Acknowledgments

This work has been supported by the Swedish Gasification Center and the Chalmers Energy Area of Advance.

References

- [1] A. Bridgwater, Renewable fuels and chemicals by thermal processing of biomass, *Chem. Eng. J.* 91 (2003) 87–102, [http://dx.doi.org/10.1016/S1385-8947\(02\)00142-0](http://dx.doi.org/10.1016/S1385-8947(02)00142-0).
- [2] A. Demirbas, Progress and recent trends in biofuels, *Prog. Energy Combust. Sci.* 33 (2007) 1–18, <http://dx.doi.org/10.1016/j.pecs.2006.06.001>.
- [3] L. Tock, M. Gassner, F. Maréchal, Thermochemical production of liquid fuels from biomass: thermo-economic modeling, process design and process integration analysis, *Biomass Bioenergy* 34 (2010) 1838–1854, <http://dx.doi.org/10.1016/j.biombioe.2010.07.018>.
- [4] W. Torres, S.S. Pansare, J.G. Goodwin, Hot gas removal of tars, ammonia, and hydrogen sulfide from biomass gasification gas, *Catal. Rev.* 49 (2007) 407–456, <http://dx.doi.org/10.1080/01614940701375134>.
- [5] C. Li, K. Suzuki, Tar property, analysis, reforming mechanism and model for biomass gasification—an overview, *Renew. Sustain. Energy Rev.* 13 (2009) 594–604, <http://dx.doi.org/10.1016/j.rser.2008.01.009>.
- [6] Z. Abu El-Rub, E.A. Bramer, G. Brem, Review of catalysts for tar elimination in biomass gasification processes, *Ind. Eng. Chem. Res.* 43 (2004) 6911–6919, <http://dx.doi.org/10.1021/ie0498403>.
- [7] Y. Shen, K. Yoshikawa, Recent progresses in catalytic tar elimination during biomass gasification or pyrolysis—a review, *Renew. Sustain. Energy Rev.* 21 (2013) 371–392, <http://dx.doi.org/10.1016/j.rser.2012.12.062>.
- [8] J. Corella, M.P. Aznar, J. Delgado, M.P. Martínez, J.L. Aragües, The deactivation of tar cracking stones (dolomites, calcites, magnesites) and of commercial methane steam reforming catalysts in the upgrading of the exit gas from steam fluidized bed gasifiers of biomass and organic wastes, *Stud. Surf. Sci. Catal.* 68 (1991) 249–252, [http://dx.doi.org/10.1016/S0167-2991\(08\)62640-3](http://dx.doi.org/10.1016/S0167-2991(08)62640-3).
- [9] R.L. Bain, D.C. Dayton, D.L. Carpenter, S.R. Czernik, C.J. Feik, R.J. French, et al., Evaluation of catalyst deactivation during catalytic steam reforming of biomass-derived syngas, *Ind. Eng. Chem. Res.* 44 (2005) 7945–7956, <http://dx.doi.org/10.1021/ie050098w>.
- [10] F. Lind, M. Seemann, H. Thunman, Continuous catalytic tar reforming of biomass derived raw gas with simultaneous catalyst regeneration, *Ind. Eng. Chem. Res.* 50 (2011) 11553–11562, <http://dx.doi.org/10.1021/ie200645s>.
- [11] M. Keller, H. Leion, T. Mattisson, H. Thunman, Investigation of natural and synthetic bed materials for their utilization in chemical looping reforming for tar elimination in biomass-derived gasification gas, *Energy Fuels* 28 (2014) 3833–3840, <http://dx.doi.org/10.1021/ef500369c>.
- [12] F. Lind, N. Berguerand, M. Seemann, H. Thunman, Ilmenite and nickel as catalysts for upgrading of raw gas derived from biomass gasification, *Energy Fuels* 27 (2013) 997–1007, <http://dx.doi.org/10.1021/ef302091w>.
- [13] F. Lind, M. Israelsson, M. Seemann, H. Thunman, Manganese oxide as catalyst for tar cleaning of biomass-derived gas, *Biomass Convers. Biorefin.* 2 (2012) 133–140, <http://dx.doi.org/10.1007/s13399-012-0042-6>.
- [14] N. Berguerand, F. Lind, M. Israelsson, M. Seemann, S. Biollaz, H. Thunman, Use of nickel oxide as a catalyst for tar elimination in a chemical-looping reforming reactor operated with biomass producer gas, *Ind. Eng. Chem. Res.* 51 (2012) 16610–16616, <http://dx.doi.org/10.1021/ie3028262>.
- [15] M. Keller, H. Leion, T. Mattisson, Use of CuO/MgAl₂O₄ and La_{0.8}Sr_{0.2}FeO₃/γ-Al₂O₃ in chemical looping reforming system for tar removal from gasification gas, *AIChE J.* (2015), in press.
- [16] H. Yokohawa, Phase diagrams and thermodynamic properties of zirconia based ceramics, *Key Eng. Mater.* 153–154 (1998) 37–74, <http://dx.doi.org/10.4028/www.scientific.net/KEM.153-154.37>.
- [17] S. Juutilainen, P. Simell, A. Krause, Zirconia: selective oxidation catalyst for removal of tar and ammonia from biomass gasification gas, *Appl. Catal. B Environ.* 62 (2006) 86–92, <http://dx.doi.org/10.1016/j.apcatb.2005.05.009>.
- [18] R. Bain, K. Magrini-Bair, Pilot scale production of mixed alcohols from wood, *Ind. Eng. Chem. Res.* (2014).

- [19] C.M. van der Meijden, H.J. Veringa, B.J. Vreugdenhil, B. van der Drift, Bioenergy II: scale-up of the Milena biomass gasification process, *Int. J. Chem. React. Eng.* 7 (2009), <http://dx.doi.org/10.2202/1542-6580.1898>.
- [20] N. Kaisalo, J. Kihlman, I. Hannula, P. Simell, Reforming solutions for biomass-derived gasification gas—experimental results and concept assessment, *Fuel* 147 (2015) 208–220, <http://dx.doi.org/10.1016/j.fuel.2015.01.056>.
- [21] H. Rönkkönen, E. Rikkinen, J. Linnekoski, P. Simell, M. Reinikainen, O. Krause, Effect of gasification gas components on naphthalene decomposition over ZrO_2 , *Catal. Today* 147 (2009) S230–S236, <http://dx.doi.org/10.1016/j.cattod.2009.07.044>.